Reactive ZnO/Ti/ZnO interfaces studied by hard x-ray photoelectron spectroscopy

Ronny Knut, Rebecka Lindblad, Sergey Grachev, Jean-Yvon Faou, Mihaela Gorgoi, Hakan Rensmo, Elin Sondergard, Olof Karis

Reactive ZnO/Ti/ZnO interfaces studied by hard x-ray photoelectron spectroscopy

Ronny Knut,[1,a)] Rebecka Lindblad,[1] Sergey Grachev,[3] Jean-Yvon Faou,[3] Mihaela Gorgoi,[2] Håkan Rensmo,[1] Elin Søndergård,[3] and Olof Karis[1]
[1]*Department of Physics and Astronomy, Uppsala University, Box 516, 75120 Uppsala, Sweden*
[2]*Helmholtz-Zentrum Berlin für Materialien und Energie, Albert-Einstein-Str. 15, D-12489 Berlin, Germany*
[3]*Unité Mixte CNRS/Sain-Gobain Recherche, 39 Quai Lucien Lefranc, 93303 Aubervilliers, France*

(Received 8 September 2013; accepted 9 December 2013; published online 28 January 2014)

The chemistry and intermixing at buried interfaces in sputter deposited ZnO/Ti/ZnO thin layers were studied by hard x-ray photoelectron spectroscopy. The long mean free path of the photoelectrons allowed for detailed studies of the oxidation state, band bending effects, and intrinsic doping of the buried interfaces. Oxidation of the Ti layer was observed when ZnO was deposited on top. When Ti is deposited onto ZnO, Zn Auger peaks acquire a metallic character indicating a strong reduction of ZnO at the interface. Annealing of the stack at 200 °C results in further reduction of ZnO and oxidation of Ti. Above 300 °C, oxygen transport from the bulk of the ZnO layer takes place, leading to re-oxidation of ZnO at the interface and further oxidation of Ti layer. Heating above 500 °C leads to an intermixing of the layers and the formation of a Zn_xTiO_y compound. © *2014 AIP Publishing LLC*. [http://dx.doi.org/10.1063/1.4854636]

I. INTRODUCTION

Reactive interfaces are essential for many thin film applications. In general, it is hard to investigate the state and structure of such systems since the characterization methods themselves can alter the interface. ZnO/Ti thin films are a typical example of a stack containing a highly reactive interface. Ti is an electropositive element and it has a tendency to reduce ZnO due to its lower enthalpy of oxide formation. Despite their complexity, ZnO/Ti based thin films find use in several areas. Ti forms an ohmic contact to ZnO,[1] which is indispensable for a wide range of applications exploiting the semiconducting properties of ZnO.[2] This interface can also be found in the glazing industry where a ZnO/Ti/Ag coating is used as a low emissivity infrared filter. In this case, an ultrathin Ti layer serves as an adhesion enhancer between the oxide and the noble metal.[3] In both cases, the origin of the peculiar electronic behavior and of the bonding reinforcement is under discussion.[4–6] The reduction of ZnO by Ti results in the creation of O vacancies in the ZnO, giving rise to reduced interfacial resistivity and n-doping.[4] The ZnO/Ti interface is very sensitive to annealing. Above a certain temperature, which scatters between 300 and 600 °C, a $ZnTiO_x$ compound forms at the interface. The studies published so far have been performed on rather thick (>25 nm) Ti layers allowing for techniques such as diffraction,[6] which does not provide direct information on the interface itself. Other observations were based on destructive sample preparation in order to access the interface properties[5] and the conclusions of this study were limited by the reactivity of Ti.

X-ray photoelectron spectroscopy (XPS) is a powerful nondestructive method able to retrieve not only chemical composition of a material but also the oxidation state of atoms. The laboratory XPS set-ups are usually surface sensitive as they use soft x-rays of 1.2–1.5 keV energy, limiting the probing depth to a few nanometers. Lately, the use of hard x-rays in modern synchrotron radiation facilities combined with new photoelectron detection technology extend the use of XPS as the probing depth can be varied between 1 and 20 nm.[7] Hard x-ray photoelectron spectroscopy (HAXPES) opens up the field for investigations of multilayer films and buried interfaces. Recently, the technique has been successfully applied to study the intermixing of metallic multilayers as well as chemical states at interfaces.[8–10] The present report is a detailed HAXPES study of sputter-deposited ZnO/Ti and Ti/ZnO interfaces, giving new insight on the behavior of this kind of systems. We were able to quantify the extent of ZnO reduction in as-deposited ZnO/Ti stacks and found a strong dependence on the sequence of deposition, which further impacted the chemical state and stoichiometry of the interface during annealing.

II. EXPERIMENTAL

The samples were deposited in a vacuum sputter-deposition chamber with the base pressure of 4×10^{-5} Pa. Si wafers with a native oxide were used as substrates. The chamber is equipped with three magnetrons allowing for deposition of a complete stack. For all the layers, dc-sputtering was used with Ar as a working gas. In order to obtain ZnO films, a Zn target was used in combination with flow of O_2 admixed to Ar. The oxygen flow was adjusted for the best stoichiometry of the ZnO films. The deposition rates were 1.7 nm/s for ZnO and 0.13 nm/s for Ti films. Three sample structures were grown, ZnO(50 nm)/Ti(4 nm)/ZnO(5 nm)/Mo(7 nm), ZnO(50 nm)/Ti(4 nm)/Mo(7 nm), and ZnO(50 nm)/Ti(5 nm). In the first two samples, Mo served as a capping layer to protect the Ti from oxidation in air. These two samples will be denoted ZnO/Ti/ZnO and ZnO/Ti, respectively, with the sample geometry illustrated in Fig. 1.

[a)]Electronic mail: Ronny.Knut@physics.gu.se

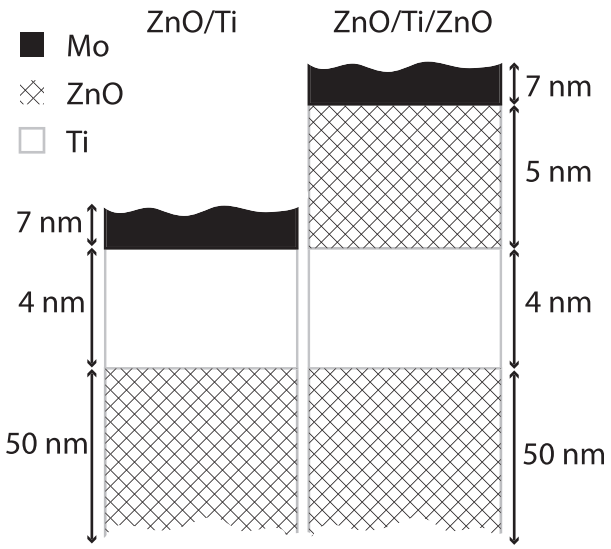

FIG. 1. The nominal sample geometry of the samples ZnO/Ti and ZnO/Ti/ZnO. Both samples are capped with Mo (filled black) and grown on 50 nm ZnO (striped black). A 4 nm Ti layer (white) is deposited on the ZnO and an additional 5 nm ZnO layer is grown on the Ti layer for sample ZnO/Ti/ZnO.

The HAXPES experiments were conducted at the KMC-1 beamline, using the HIKE end-station, at Bessy II at Helmholtz Zentrum Berlin. This beamline offers photon energies ranging between 2 and 12 keV with high resolution.[7] In all the presented data, a photon energy of 4 keV was used unless stated otherwise. This energy provides a good compromise between peak intensity, resolution, and depth sensitivity (~5 nm inelastic mean free path). The analysis chamber is equipped with an Ar^+ sputter gun which was used for sputtering the Mo cap to decrease its thickness and increase the photoelectron yield from deeper layers. The sample manipulator is equipped with a heating stage which can heat samples up to ~800 °C. The samples were heated at a rate of 20 °C/min until the required temperature, between 200 °C and 550 °C, was reached and kept there for 10 min. After each annealing step, the sample was cooled down to room temperature (RT) before the core level spectra were recorded. All spectra were energy calibrated relative to an Au reference which was in electrical contact with the samples, hence zero binding energy (BE) corresponded to the Fermi level. Pure sputter-deposited materials (Zn, ZnO, TiO_2) were also examined and used as reference samples. The change of the binding energy of a particular core level denotes the chemical shift and it depends on the chemical environment.[8,11] In particular, Ti 2p peaks exhibit large chemical shifts, while Zn 2p peaks do not.[12] Therefore, we have also measured the Zn LMM Auger which shows a distinctive difference between the metallic and oxidized states. However, the probing depth of Auger electrons is insensitive to the photon energy and restricted to a few nm, so a reasonable signal could not be obtained for all sample geometries.

III. RESULTS AND DISCUSSION

Fig. 2(a) shows the Ti 2p spectrum of a reference TiO_2 sample obtained at 4 keV photon energy. This spectrum

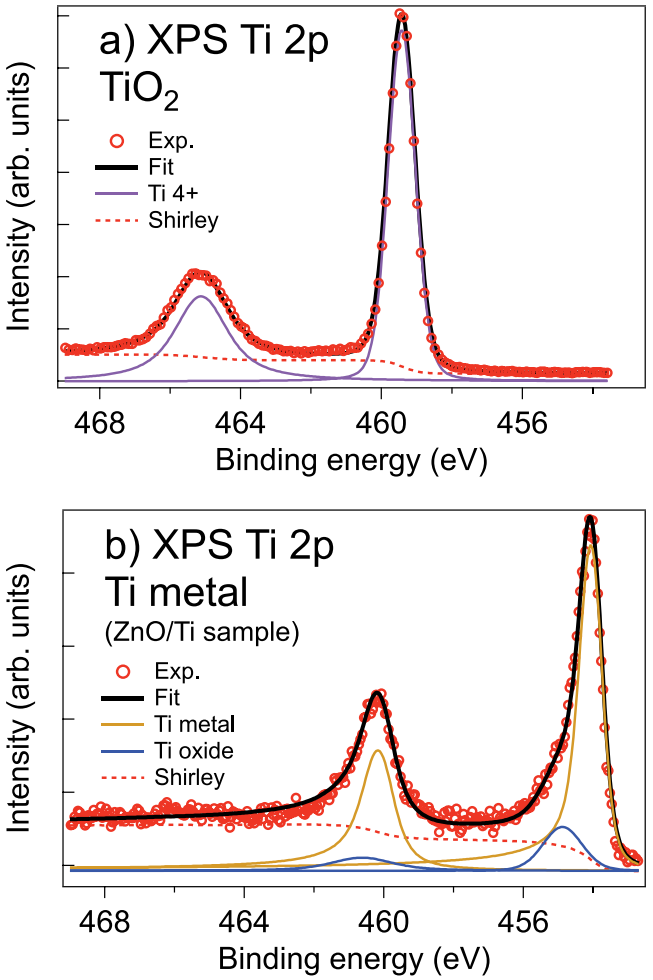

FIG. 2. (a) Ti 2p spectrum of TiO_2 recorded with 4 keV photon energy. A good fit is obtained using a single peak for each spin orbit split core level corresponding to $Ti^{4+}_{3/2,1/2}$. (b) Ti 2p spectrum of ZnO/Ti sample recorded with 4 keV photon energy. The sample contains mainly metallic Ti^0. A weak oxidation is found which is represented by the blue spectra.

corresponds to Ti^{4+} where the core level is spin-orbit split by 5.7 eV (Ref. 12) into $Ti^{4+}_{3/2}$ (459.4 eV BE) and $Ti^{4+}_{1/2}$. A good fit is obtained by a single peak at both spin orbit split levels with a Gaussian broadening of 0.83 eV convoluted with a Lorenzian broadening of 0.22 eV and 1.4 eV for the $Ti^{4+}_{3/2}$ and $Ti^{4+}_{1/2}$ peaks, respectively. The Lorenzian broadening is a lifetime effect of the core hole. The $Ti^{4+}_{1/2}$ core hole has an additional decay channel, the Coster-Kroenig transition,[13] which shortens its lifetime and hence increases the Lorenzian broadening compared to the $Ti^{4+}_{3/2}$ core hole. The Gaussian broadening of 0.83 eV accounts for the experimental resolution (0.35 eV in the present experiments) but also suggest some degree of disorder in the film. A Shirley background (red dotted line in Fig. 2(a)) is included in all fittings of spectra.[14] The Ti 2p spectrum for the ZnO/Ti sample, as deposited, is presented in Fig. 2(b). This spectrum shows a reasonably good fit by using a Doniach-Sunjic line profile (brown) which is appropriate for metallic systems.[15] The spin orbit splitting for the metallic Ti is 6.12 eV, in accordance with literature.[12] The Doniach-Sunjic profile is convoluted with a Gaussian broadening of 0.62 eV and exhibits an asymmetry parameter of 0.1 and Lorenzian widths of

0.22 eV and 0.65 eV for the $Ti^0_{3/2}$ (454.1 eV BE) and $Ti^0_{1/2}$ peaks, respectively. There is also a weak doublet represented by the blue peaks which corresponds to slightly oxidized Ti. This oxidation is due to the chemical reaction of Ti with ZnO at the interface.

Unlike the ZnO/Ti, the ZnO/Ti/ZnO sample shows a high extent of Ti oxidation before annealing, Fig. 3. This spectrum shows not only a large amount of Ti^{4+} but also a significant amount of lower oxidation states. The BE positions of Ti^{3+} and Ti^{2+} correspond well with literature values.[12] The BE of the metallic peak is approximately 0.4 eV higher than for the metallic peak in Fig. 2(b) indicating that the electronic structure of the thin layer of metallic Ti is affected by the interface to the oxide.[8,11]

Fig. 4(a) shows the Ti 2p core levels after annealing at different temperatures for the ZnO/Ti sample. The RT spectrum which was presented in Fig. 2(b) is also shown here for comparison. The dotted lines correspond to the BE of Ti oxidation states (4+, 3+, 2+, 0) from high to low BE, respectively. After annealing at 200 °C, we observe a large increase of Ti^{2+}, indicating oxidation of Ti due to oxygen from ZnO. The oxidation of Ti is further advanced at higher annealing temperature and after annealing at 550 °C the Ti layer is almost completely oxidized to Ti^{4+}. We also show a spectrum obtained with 2 keV photon energy after 550 °C annealing (red dotted line). This spectrum shows a higher contribution from non- or low-oxidation components than the spectrum recorded at 4 keV. Since lower photon energies gives a decreased probing depth, this confirms that the Ti is oxidized from below and that the oxidation is not complete close to the Mo capping layer.

Fig. 4(b) shows the temperature dependent evolution of Ti 2p in the ZnO/Ti/ZnO sample, which was largely oxidized already after deposition. For comparison, the RT spectrum from Fig. 3 is also included in Fig. 4(b). The RT spectra were obtained with both 4 keV and 2 keV photon energy. The metallic and low oxidation states are less pronounced with the 2 keV photon energy compared to the 4 keV confirming that the Ti oxide is situated closer to the surface. The metallic component has mostly disappeared after annealing

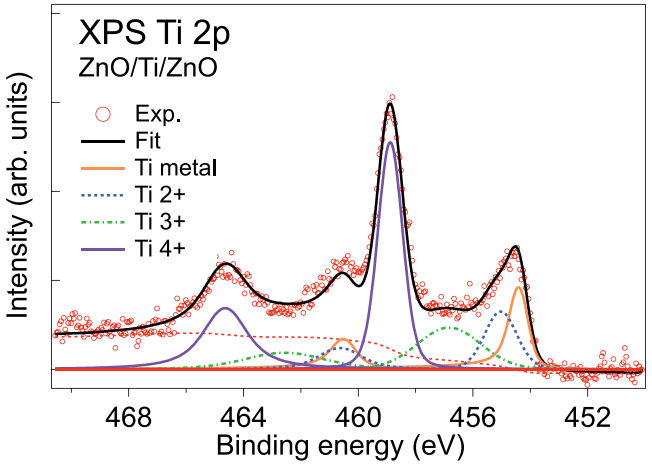

FIG. 3. Ti 2p spectrum of sample ZnO/Ti/ZnO recorded with 4 keV photon energy. The sample is highly oxidized. A weak metallic contribution is still present but the main Ti contribution corresponds to Ti^{4+} as in TiO_2.

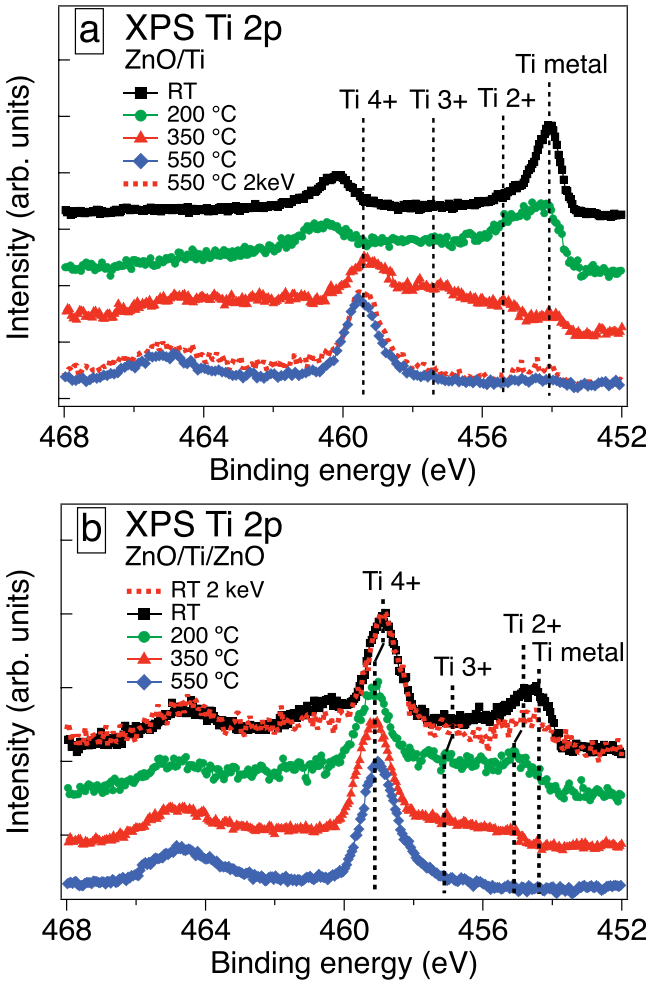

FIG. 4. Ti 2p spectra after annealing. The vertical dotted lines mark the binding energy of Ti oxidation states (4+, 3+, 2+, 0). (a) ZnO/Ti sample. The strong metallic component is largely oxidized already after annealing at 200 °C. A weak metallic component is observed after 550 °C using 2 keV, suggesting that the oxidation is not complete close to the Mo interface. (b) ZnO/Ti/ZnO sample. The initially weak metallic component is almost completely lost after annealing at 200 °C. The higher contribution of oxidized Ti when using 2 keV photon energy at RT suggests an initial oxidation mainly from the top ZnO layer.

at 200 °C. The oxidation state is almost completely Ti^{4+} after annealing at 550 °C. The vertical black dotted lines correspond to rigid BE differences between the oxidized components and it is found that the Ti^{4+} component shifts after annealing. It is also found that the Ti^{4+} in the ZnO/Ti/ZnO sample has 0.3 eV lower BE than in the ZnO/Ti sample after annealing. This could be due to band bending effects since the Ti-oxides have close contact with the Mo metal in the ZnO/Ti sample.

A quantitative estimation of the equivalent thickness of metallic Ti, assuming layered structures, is presented in Fig. 5. The amount of the metallic component is derived by assuming a nominal Ti layer of 4 nm and comparing the area of Ti 2p oxide and metallic peaks after a peak fit of the spectra in Figs. 4(a) and 4(b). The probing depth effect is accounted for by assuming that TiO_x is formed in the lower (closer to the substrate) part of the Ti layer. For the ZnO/Ti/ZnO sample, an additional oxidation from the top (closer to the surface) is accounted for. The error bars

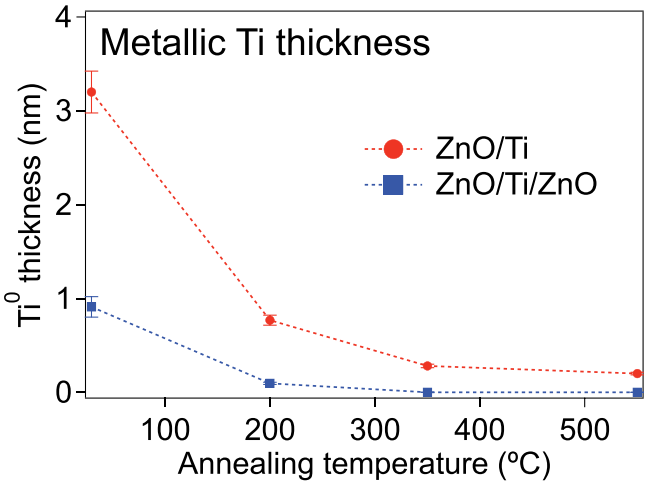

FIG. 5. Estimated thickness of metallic Ti after annealing, obtained from Figs. 4(a) and 4(b). The Ti is very sensitive to oxidation from the ZnO layer already after heat treatment at 200 °C.

correspond to an uncertainty in separating the metallic and the low oxidation state of Ti. According to Fig. 5, before annealing, a ~1 nm thick oxide layer is formed at the lower interface while at the top interface (only sample ZnO/Ti/ZnO), a ~2 nm oxidized Ti layer is formed, resulting in a ~1 nm thick metallic Ti component for sample ZnO/Ti/ZnO and a 3 nm thick metallic component for sample ZnO/Ti before annealing. After annealing at 200 °C, the Ti in the ZnO/Ti/ZnO sample is almost fully oxidized. A metallic Ti layer of ~1 nm still remains in the ZnO/Ti sample, in which the oxidized Ti is mostly in a low oxidation state.

The O 1s and Zn $2p_{3/2}$ core level peaks for the ZnO/Ti sample are shown in Figs. 6(a) and 6(b), respectively. Background intensities, obtained from survey spectra (not shown), are used for normalization such that the intensities of different core level intensities can be compared without considering variations in the synchrotron ring current, i.e., photon intensities. These backgrounds are relatively unaffected by annealing which also ensures that core level intensities can be compared between different annealing temperatures. The O 1s at RT shows a distinct double peak feature where the peak at high BE (~532 eV) likely comes from oxygen on the Mo surface, while the peak around 530 eV BE is due to oxygen in the ZnO layer. The vertical black dotted lines in both Figs. 6(a) and 6(b) correspond to the BE position of O 1s and Zn $2p_{3/2}$, respectively for n-doped ZnO and they are also close to the BE positions of metallic Zn $2p_{3/2}$ and O 1s usually found in TiO_2.[12,16–18] Both the Zn $2p_{3/2}$ and O 1s exhibit broadened peaks at RT which is probably a consequence of two effects. The reduction of ZnO, due to the Ti layer, will likely create a gradient of intrinsic doping close to the interface which will be manifested as line broadening. Also, the broadening can be induced by the band bending often found in metal/semiconductor interfaces leading to a Schottky barrier at the interface. Although ZnO/Ti usually form an ohmic contact, this does not ensure that band bending is absent.[19]

The area of the O 1s peak increases as the sample is annealed, indicating a diffusion of oxygen towards the

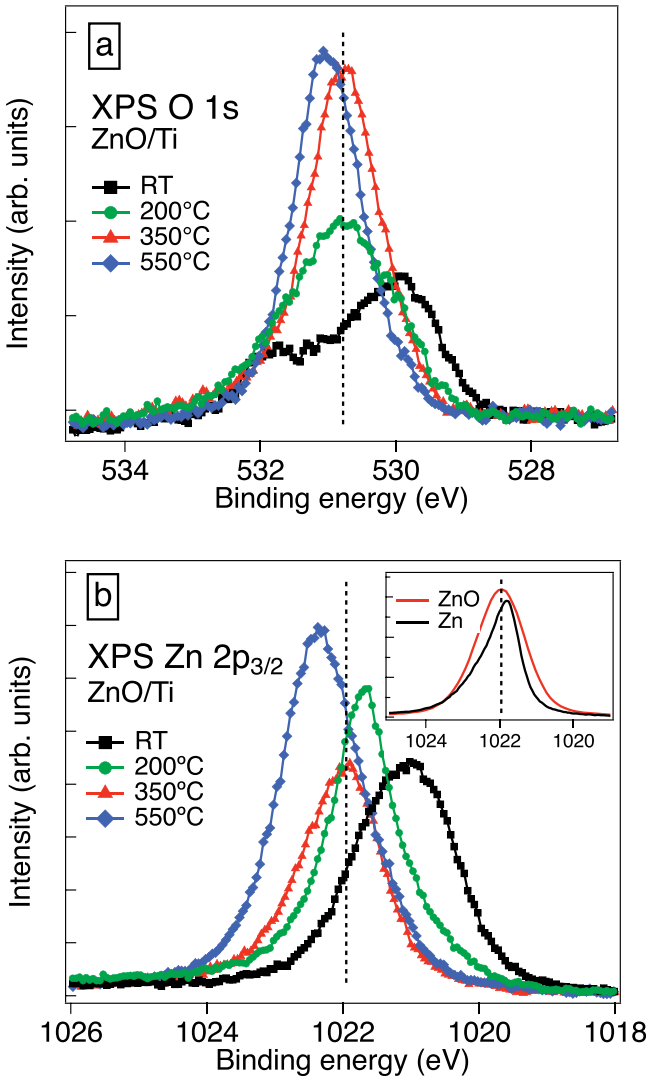

FIG. 6. (a) XPS of O 1s in the ZnO/Ti sample. A large intensity increase is observed after annealing to 350 °C which is consistent with oxygen diffusion towards the surface. (b) XPS of Zn $2p_{3/2}$ shows similar shifts as the O 1s indicating changes in the Fermi level. After annealing to 200 °C, an enhanced metallic component is observed. The insert shows the peak shapes for Zn $2p_{3/2}$ in ZnO and metallic Zn.

sample surface. Both O 1s and Zn $2p_{3/2}$ show similar BE shifts as the sample is annealed, which indicates changes in the Fermi level of ZnO due to increased intrinsic n-doping, likely due to the formation of oxygen vacancies. However, the BE and peak shape of Zn $2p_{3/2}$ after annealing at 200 °C have a strong resemblance to metallic Zn (referred to as the Zn^0 component from here on), compare to inset in Fig. 6(b) which shows the Zn $2p_{3/2}$ for reference ZnO and metallic Zn samples. This change in oxidation state of Zn also explains the difference in BE shift between Zn $2p_{3/2}$ and O 1s at this annealing temperature. Further evidence of the presence of the Zn^0 component will be given below where we study the Zn Auger LMM spectra. After annealing at 350 °C, we observe an increase of the O 1s area which corresponds to the strong oxidation of Ti. At this temperature, oxygen from the ZnO bulk begins to diffuse towards the surface, which also results in oxidation of the Zn^0 component found after annealing at 200 °C. The Zn $2p_{3/2}$ area shows a strong

increase after annealing at 550 °C which indicates that the ZnO and Ti/TiO_2 are intermixing. The BE have become higher than found for highly n-doped ZnO (black dotted line) which indicates that a new compound has formed.

Comparing the area ratios between different atomic components, as a function of annealing temperature, provides additional information about the diffusion. In Figs. 7(a) and 7(b), we have plotted the ratio between Ti $2p_{3/2}$ and Zn $2p_{3/2}$ areas and the Zn $2p_{3/2}$ and O 1s areas, respectively. The differences in cross section were taken in consideration and the surface component was subtracted from the O 1s peak. The error bars in both Figs. 7(a) and 7(b) are due to the uncertainty in normalizing the core-level intensities to the same photon exposure. Also, an additional error source is included for sample ZnO/Ti in Fig. 7(b) due to the uncertainty of separating the bulk and surface component of oxygen. The Ti/Zn ratios have been normalized to the value obtained before annealing (Fig. 7(a)). The ZnO/Ti sample (red circles) show a dip of the Ti/Zn ratio at 200 °C which could be related to the formation of Zn^0 at 200 °C. However,

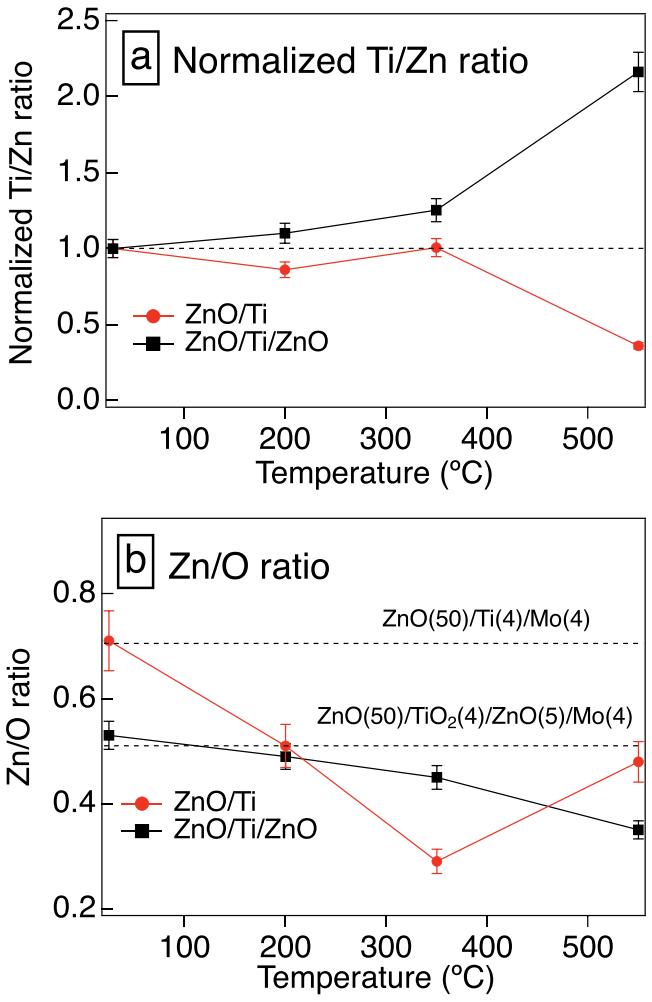

FIG. 7. (a) The ratio between Ti $2p_{3/2}$ and Zn $2p_{3/2}$ for both ZnO/Ti (red circles) and ZnO/Ti/ZnO (black squares) samples. Both samples are normalized at the ratio obtained at RT. (b) The ratio between Zn $2p_{3/2}$ and O 1s for both ZnO/Ti (red circles) and ZnO/Ti/ZnO (black squares) samples. The top and bottom horizontal black dotted lines corresponds to calculated Zn/O ratios of stoichiometric ZnO in ZnO/Ti/Mo and $ZnO/TiO_2/ZnO/Mo$, respectively.

the ratio regains its initial value at 350 °C, which indicates that the Zn and Ti do not intermix at this temperature and that the main interlayer diffusion is due to oxygen. The ZnO/Ti/ZnO sample shows a generally increasing Ti/Zn ratio with annealing temperature, which indicates that Ti is mixing with the top ZnO layer even for low annealing temperatures. At 550 °C, the Ti/Zn ratio strongly deviates from ~1 which suggests a strong intermixing between ZnO and Ti for both samples.

We have calculated the Zn/O ratio corresponding to the two sample geometries, ZnO(50 nm)/Ti(4 nm)/Mo(4 nm) and $ZnO(50\,nm)/TiO_2(4\,nm)/ZnO(5\,nm)/Mo(4\,nm)$. The values are plotted in Fig. 7(b) as two horizontal black dotted lines at the top and bottom, respectively. The inelastic mean free paths for photoelectrons corresponding to O1s and Zn 2p were calculated with the QUASES software.[20] From the photoemission spectra of Mo 3d (not shown), we estimate that a 4 nm thick Mo film remained after the initial Ar^+ sputtering of the stacks. The Zn/O ratio for the as deposited ZnO/Ti sample corresponds well to the calculated value of stoichiometric ZnO, in accordance with a weak oxidation of the Ti layer. The oxygen diffusion into Ti decreases the ratio as the sample is annealed at 350 °C. As suggested above, ZnO and Ti form a new compound at 550 °C, where the Zn/O ratio approaches a ratio of 1:2. The valency of Ti evolves towards 4+ suggesting the formation of a Zn_2TiO_4 spinel.[21] X-ray diffraction studies (not shown) indicate the formation of new nanocrystalline phases but the peaks are too broad to conclusively confirm a spinel structure.

The ZnO/Ti/ZnO sample showed highly oxidized Ti, Fig. 4(b), which corresponds well with the lower black dotted line in Fig. 7(b) that indicates the calculated Zn/O ratio of $ZnO(50\,nm)/TiO_2(4\,nm)/ZnO(5\,nm)/Mo(4\,nm)$. The Zn $2p_{3/2}$ and O 1s (not shown) have BE corresponding to n-doped ZnO (that is, corresponding to the vertical black dotted lines in Figs. 6(a) and 6(b)) and do not exhibit any BE shifts, nor significant line broadening, as the sample is heated. Since the main contribution to the core level intensities comes from the top ZnO layer, the upper part appears inert upon annealing. The Zn $2p_{3/2}$ intensity remains constant up to 350 °C while the O 1s continuously increases which results in the decrease of the Zn/O ratio (black squares in Fig. 7(b)). This suggests that the initial oxidation is a consequence of the top ZnO layer deposition while the oxidation during annealing is due to the oxygen diffusion from the bottom ZnO layer.

We were not able to record the Zn LMM Auger spectra from samples protected with a Mo cap due to the limited probing depth of Auger electrons. Instead, the Zn LMM Auger spectra were measured on a ZnO(50 nm)/Ti(5 nm) sample without a capping layer as presented in Fig. 8. Even though the Ti layer has been directly exposed to ambient air, HAXPES indicates a significant amount of metallic Ti below the oxidized surface layer. The two peaks in the Auger spectra, marked by dotted lines, both appear in a reference spectrum of metallic Zn (not shown) while only the peak at lower kinetic energy is pronounced in the Zn LMM spectra of ZnO. The intensity ratio of these two peaks after annealing is plotted in the inset of Fig. 8 (red dotted line). The horizontal

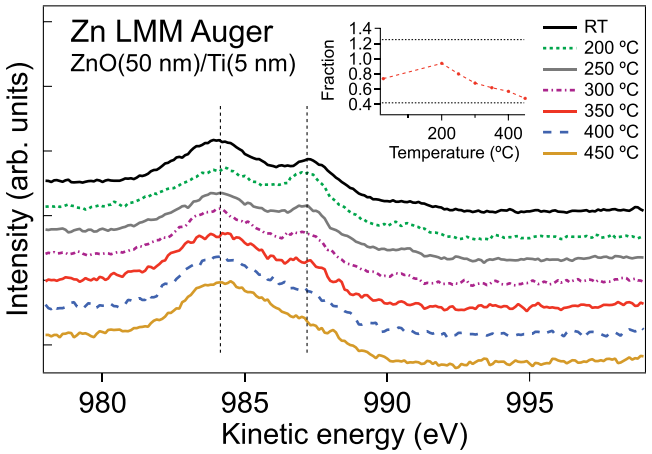

FIG. 8. Zn LMM Auger spectra of ZnO(50 nm)/Ti(5 nm) with no capping layer. The peak around 987 eV kinetic energy is characteristic to metallic Zn. The deposition of Ti on ZnO clearly leads to a reduction of ZnO. The inset shows the intensity ratio Zn/ZnO at the kinetic energies represented by the dotted lines in the main figure. The top and bottom dotted lines in the insert correspond to values obtained from reference metallic Zn and ZnO samples, respectively.

top and bottom black dashed lines in the inset indicate the ratio for the metallic Zn and ZnO samples, respectively. The ZnO is reduced by the top Ti layer in the as deposited sample and becomes even more reduced as the oxygen is diffusing from the ZnO into the Ti after annealing at 200 °C. For temperatures above 200 °C, the oxygen from the ZnO bulk diffuses towards the surface and oxidizes the reduced Zn at the interface. This corresponds well with the observed line shapes of Zn $2p_{3/2}$ in Fig. 6(b) which showed a strong Zn^0 component after annealing at 200 °C.

IV. SUMMARY AND CONCLUSION

We can summarize our results as follows: Fig. 9 (left) shows the actual sample geometry before annealing in contrast to the designed stack shown in Fig. 1. The as-deposited layers contained a certain amount of Ti oxide. In the case of ZnO deposited onto a Ti layer, the oxidation occurred during exposure of Ti to the reactive oxygen plasma (Fig. 4(b)). When Ti was deposited onto ZnO, we observed a metallic component of Zn, reflecting the formation of O vacancies (Figs. 4(a) and 8) confirming the suggestion of earlier publications.[4] The extent of the ZnO reduction was limited to the near proximity of the as-deposited interface. This chemical reaction extended further during annealing at 200 °C, as a stronger metallic component of the Zn peak was observed. This could explain the decrease of interface resistance reported by some authors.[4–6] At the same time, a thicker TiO_x layer was formed suggesting the reduction of ZnO by Ti at the interface. Annealing at 350 °C resulted in re-oxidation of the reduced ZnO at the interface and a deeper oxidation of the Ti layer. It suggests that the bulk diffusion of oxygen was activated at this temperature. It is well known that sputter-deposited films contain a large amount of structural and chemical defects. These defects can cause large residual stresses. A previous study of the residual stress in similar ZnO layers showed that a vast stress relaxation occurred at around 300 °C (Ref. 22) which was attributed to structural reorganization of the film and defect repair. Other authors evoked the apparent increase of oxygen diffusion as being induced by the onset of diffusion of H and OH groups present in sputtered ZnO.[23,24] At 550 °C oxygen, Zn and Ti atoms all become mobile and interdiffusion drives the formation of a new compound. Presumably, in the ZnO/Ti/ZnO stack, a similar scenario occurs at the lower interface. However, the Ti oxidation is much more pronounced in the as-deposited film due to the top ZnO. Fig. 9 (right) is a schematic presentation of the films after annealing. Apparently, the two interfaces, Ti/ZnO and ZnO/Ti, behave differently during annealing. In addition to the differences in their structure and initial conditions discussed above, the rate of inter-diffusion and oxygen exchange can be influenced by asymmetric intermixing as observed for other systems.[25–28]

In conclusion, HAXPES was successfully used to probe ZnO/Ti interfaces in multilayers. It provided a detailed view of the composition and the oxidation state of Ti and Zn atoms close to the interface in as-deposited films and after annealing. The results unveil a strong deviation between the stacks as-designed, as-deposited and after annealing due to the reactivity of the Ti layer, Figs. 1 and 9. The order of

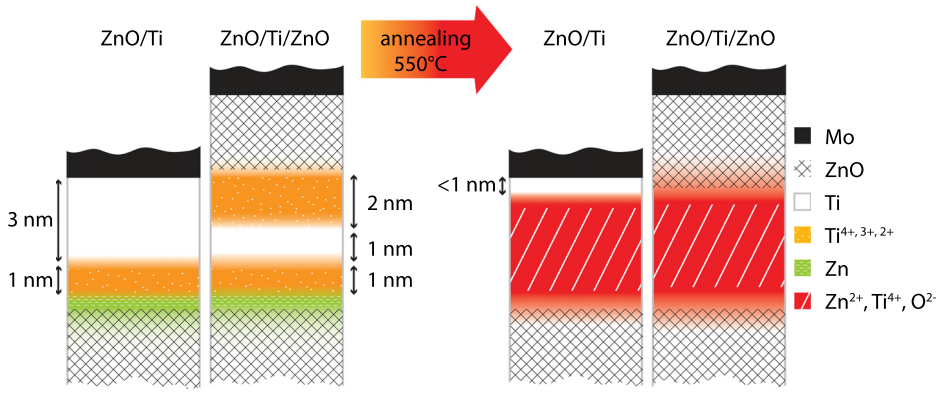

FIG. 9. Actual sample geometry of ZnO/Ti and ZnO/TiZnO samples, both in as-deposited (left) and after annealing to 550 °C (right). In the as-deposited samples, an oxidation of Ti is found at both the ZnO/Ti and Ti/ZnO interfaces. When the Ti is deposited on ZnO, a metallic character of Zn is formed due to reduction of ZnO at the interface. The figure illustrates the location of Zn rather than the formation of a continuous layer. After annealing to 550 °C, a weak Ti metallic component still exist in the ZnO/Ti sample but the majority of the Ti has intermixed with the ZnO.

deposition proved to be an important parameter impacting both the room temperature structure and the reaction kinetics upon annealing. These results clearly demonstrate the power of HAXPES to probe the link between processing conditions and the internal structure of complex multilayered stacks.

ACKNOWLEDGMENTS

We acknowledge the Helmholtz-Zentrum Berlin for provision of synchrotron radiation beamtime at beamline KMC-1 of BESSY II. The research leading to these results has received funding from the European Community's Seventh Framework Programme (FP7/2007-2013) under Grant Agreement No. 312284. The authors also gratefully acknowledge funding from the Swedish Energy Agency, the Swedish Resarch Council (VR) and StandUp for Energy.

[1]K. Ip, K. H. Baik, Y. W. Heo, D. P. Norton, S. J. Pearton, J. R. LaRoche, B. Luo, F. Ren, and J. M. Zavada, "Annealing temperature dependence of contact resistance and stability for ti/al/pt/au ohmic contacts to bulk n-zno," J. Vac. Sci. Technol. B **21**(6), 2378–2381 (2003).
[2]U. Ozgur, Y. I. Alivov, C. Liu, A. Teke, M. A. Reshchikov, S. Dogan, V. Avrutin, S.-J. Cho, and H. Morkoc, "A comprehensive review of zno materials and devices," J. Appl. Phys. **98**(4), 041301 (2005).
[3]S. Grachev, A. Mehlich, J.-D. Kamminga, E. Barthel, and E. Søndergård, "High-throughput optimization of adhesion in multilayers by superlayer gradients," Thin Solid Films **518**(21), 6052–6054 (2010).
[4]H. S. Yang, D. P. Norton, S. J. Pearton, and F. Ren, "Ti/au n-type ohmic contacts to bulk zno substrates," Appl. Phys. Lett. **87**(21), 212106 (2005).
[5]J. Chen, T. Anderson, S. Jang, F. Ren, Y. Li, H.-S. Kim, B. Gila, D. Norton, and S. Pearton, "Ti/au ohmic contacts to al-doped n-zno grown by pulsed laser deposition," J. Electrochem. Soc. **153**(5), G462–G464 (2006).
[6]H.-K. Kim, S.-H. Han, T.-Y. Seong, and W.-K. Choi, "Electrical and structural properties of ti/au ohniic contacts to n-zno," J. Electrochem. Soc. **148**(3), G114–G117 (2001).
[7]M. Gorgoi, S. Svensson, F. Schäfers, G. Öhrwall, M. Mertin, P. Bressler, O. Karis, H. Siegbahn, A. Sandell, H. Rensmo, W. Doherty, C. Jung, W. Braun, and W. Eberhardt, "The high kinetic energy photoelectron spectroscopy facility at bessy progress and first results," Nucl. Instrum. Methods Phys. Res. A **601**(1–2), 48–53 (2009).
[8]S. Granroth, R. Knut, M. Marcellini, G. Andersson, S. Svensson, O. Karis, M. Gorgoi, F. Schäfers, W. Braun, W. Eberhardt, W. Olovsson, E. Holmström, and N. Mårtensson, "Investigation of interface properties of ni/cu multilayers by high kinetic energy photoelectron spectroscopy," Phys. Rev. B **80**(9), 094104 (2009).
[9]R. Knut, P. Svedlindh, O. Mryasov, K. Gunnarsson, P. Warnicke, D. Arena, M. Björck, A. Dennison, A. Sahoo, S. Mukherjee, D. Sarma, S. Granroth, M. Gorgoi, and O. Karis, "Interface characterization of co2mnge/rh2cusn heusler multilayers," Phys. Rev. B **88**(13), 134407 (2013).
[10]M. Sing, G. Berner, K. Goß, A. Müller, A. Ruff, A. Wetscherek, S. Thiel, J. Mannhart, S. Pauli, C. Schneider, P. Willmott, M. Gorgoi, F. Schäfers, and R. Claessen, "Profiling the interface electron gas of laalo3/srtio3 heterostructures with hard x-ray photoelectron spectroscopy," Phys. Rev. Lett. **102**(17), 176805 (2009).
[11]B. Johansson and N. Mårtensson, "Core-level binding-energy shifts for the metallic elements," Phys. Rev. B **21**, 4427–4457 (1980).
[12]M. Biesinger, L. Lau, A. Gerson, and R. Smart, "Resolving surface chemical states in XPS analysis of first row transition metals, oxides and hydroxides: Sc, Ti, V, Cu and Zn," Appl. Surf. Sci. **257**(3), 887–898 (2010).
[13]D. Coster and R. D. L. Kronig, "New type of auger effect and its influence on the x-ray spectrum," Physica **2**(1–12), 13–24 (1935).
[14]J. Végh, "The shirley background revised," J. Electron Spectrosc. Relat. Phenom. **151**, 159–164 (2006), and references therein.
[15]S. Doniach and M. Sunjic, "Many-electron singularity in x-ray photoemission and x-ray line spectra from metals," J. Phys. C **3**(2), 285 (1970).
[16]C.-T. Wang and J.-C. Lin, "Surface nature of nanoparticle zinc-titanium oxide aerogel catalysts," Appl. Surf. Sci. **254**, 4500–4507 (2008).
[17]D. Iusan, R. Knut, B. Sanyal, O. Karis, O. Eriksson, V. Coleman, G. Westin, J. Wikberg, and P. Svedlindh, "Electronic structure and chemical and magnetic interactions in zno doped with co and al: Experiments and ab initio density–functional calculations," Phys. Rev. B **78**(8), 085319 (2008).
[18]R. Knut, J. Wikberg, K. Lashgari, V. Coleman, G. Westin, P. Svedlindh, and O. Karis, "Magnetic and electronic characterization of highly co-doped zno: An annealing study at the solubility limit," Phys. Rev. B **82**(9), 094438 (2010).
[19]L. J. Brillson and Y. Lu, "Zno schottky barriers and ohmic contacts," J. Appl. Phys. **109**(12), 121301 (2011).
[20]S. Tougaard: QUASES-IMFP-TPP2M. Software packages to characterize surface nano-structures by analysis of electron spectra, see http://www.quases.com/products/quases-imfp-tpp2m/.
[21]U. Steinike and B. Wallis, "Formation and structure of ti-zn-oxides," Cryst. Res. Technol. **32**(1), 187–193 (1997).
[22]P. Renault, C. Krauss, E. L. Bourhis, G. Geandier, A. Benedetto, S. Grachev, and E. Barthel, "In situ thermal residual stress evolution in ultra-thin zno and ag films studied by synchrotron x-ray diffraction," Thin Solid Films **520**(5), 1390–1394 (2011).
[23]E. V. Monakhov, A. Y. Kuznetsov, and B. G. Svensson, "Zinc oxide: bulk growth, role of hydrogen and schottky diodes," J. Phys. D: Appl. Phys. **42**(15), 153001 (2009).
[24]G. A. Shi, M. Saboktakin, M. Stavola, and S. J. Pearton, "'Hidden hydrogen' in as-grown zno," Appl. Phys. Lett. **85**(23), 5601–5603 (2004).
[25]P. Süle, M. Menyhárd, L. Kótis, J. Lábár, and W. F. Egelhoff, "Asymmetric transient enhanced intermixing in pt/ti," J. Appl. Phys. **101**(4), 043502 (2007).
[26]G. Sharma, R. Gupta, and A. Gupta, "Study of interfacial modification in fe/ag multilayer with thermal annealing using x ray standing wave," AIP Conf. Proc. **1349**(1), 661–662 (2011).
[27]Q. Zhong, Z. Zhang, S. Ma, R. Qi, J. Li, Z. Wang, P. Jonnard, K. L. Guen, and J.-M. André, "Thermally induced structural modification in the al/zr multilayers," Appl. Surf. Sci. **279**, 334–342 (2013).
[28]A. Gupta, D. Kumar, and V. Phatak, "Asymmetric diffusion at the interfaces in fe/si multilayers," Phys. Rev. B **81**, 155402 (2010).